Ferroelectrics, 2001, Vol. 251, pp. 191-198
Reprints available directly from the publisher
Photocopying permitted by license only

Effect of Defect Induced Nucleation and Growth on Switching Behavior in Ferroelectrics

RAJEEV AHLUWALIA and WENWU CAO

Materials Research Laboratory, The Pennsylvania State University, University Park, Pennsylvania 16802

(Received June 2, 2000)

The switching behavior in ferroelectrics has been simulated using a time-dependent-Ginzburg-Landau approach, incorporating the contributions of dipolar defects. The model also includes the coupling with elastic fields. The dipolar defects are simulated by an inhomogeneous electric field produced by these localized dipoles. Domain pattern evolution was simulated with the sudden application/removal of the external bias electric field. We found that due to defect induced nucleation, a multi-domain twinned state is stabilized when the external electric field is removed from a poled single domain state. On the application of field in the opposite direction, the twinned state can be switched to a single domain with reverse polarization. The associated switching current has also been calculated.

Keywords: polarization switching; domain pattern; dipolar defects; switching current; time dependent Ginzgurg-Landau

INTRODUCTION

When a strong enough external electric field is applied to a ferroelectric material, the spontaneous polarization can be switched to the reverse direction. It is crucial to understand the mechanism of this switching process for many applications of ferroelectric materials. It has been recognized that the switching process is influenced by the presence of defects, which are present in the form of vacancies and charged

dopants [1]. These defects may act as nucleation sites for domains of other orientations, which trigger the switching process and reduce the observed coercive field.

The classical picture for the polarization switching is via 180° domain reorientation[1]. There have been some simulation studies recently attempting to quantify the domain behavior during switching in ceramics and single crystals[2, 3], but those models are limited to perfect systems. Because the experimentally observed coercive field is always much smaller than the theoretical value, a realistic model must take into account the effect of defects, as well as the influence of elastic strain coupling.

The time-dependent Ginzburg-Landau (TDGL) formalism has been shown to be an extremely useful tool in the study of dynamics of phase transitions. The TDGL equations have been used to study pattern formation in defect free ferroelectrics having 90° domain walls[4, 5]. In this paper, we report a simulation study of polarization switching in ferroelectrics, based on the TDGL approach, specifically addressing the issue of nucleation from localized dipolar defects and with the influence of elastic long range interaction. Here, we focus on the time evolution of the domain patterns during switching. A detailed study of the hysteresis loops will be reported elsewhere [6].

THE MODEL

The Ginzburg-Landau free-energy for ferroelectric systems has been given before[7, 3]. In this work, we restrict to a 2-d system undergoing a square to rectangle transition. The total free-energy is written as

$$F = \int d\vec{r}[f_l + f_g + f_{el} + f_{es} + f_{ext} + f_d] \tag{1}$$

where f_l is the local free-energy density given by

$$f_l = \frac{\alpha_1}{2}({P_x}^2 + {P_y}^2) + \frac{\alpha_{11}}{4}({P_x}^4 + {P_y}^4) + \frac{\alpha_{12}}{2}{P_x}^2{P_y}^2, \tag{2}$$

f_g is the gradient energy,

$$f_g = \frac{g_1}{2}\left[\left(\frac{\partial P_x}{\partial x}\right)^2 + \left(\frac{\partial P_y}{\partial y}\right)^2\right] + \frac{g_2}{2}\left[\left(\frac{\partial P_x}{\partial y}\right)^2 + \left(\frac{\partial P_y}{\partial x}\right)^2\right] + g_3\left(\frac{\partial P_x}{\partial x}\right)\left(\frac{\partial P_y}{\partial y}\right). \tag{3}$$

It has been shown that the gradient energy can be obtained as a local approximation to the dipole-dipole interactions[11]. The term f_{el} represents the elastic energy of a system with square symmetry. We consider the bulk strain $\phi_1 = (\eta_{xx} + \eta_{yy})/\sqrt{2}$, deviatoric strain $\phi_2 = (\eta_{xx} - \eta_{yy})/\sqrt{2}$ and shear strain $\phi_3 = \eta_{xy} = \eta_{yx}$. Here $\eta_{ij} = \frac{1}{2}(\frac{\partial u_i}{\partial x_j} + \frac{\partial u_j}{\partial x_i})$ is the linear elastic strain tensor. The elastic free-energy can then be written as

$$f_{el} = \frac{a_1}{2}{\phi_1}^2 + \frac{a_2}{2}{\phi_2}^2 + \frac{a_3}{2}{\phi_3}^2, \tag{4}$$

where a_1, a_2 and a_3 are combinations of second order elastic constants. The coupling energy f_{es} may be written as,

$$f_{es} = -q_1\phi_1({P_x}^2 + {P_y}^2) - q_2\phi_2({P_x}^2 - {P_y}^2) - q_3\phi_3 P_x P_y. \tag{5}$$

Here q_1, q_2 and q_3 are constants that are related to the electrostrictive constants of the system. The term f_{ext} is given by $f_{ext} = -\vec{E}_{ext}\cdot\vec{P}$. The amplitude of field $\vec{E}_{ext}$ is a homogeneous tunable quantity for studying domain switching. The term f_d represents the free-energy contribution due to randomly distributed dipolar defects given as $f_d = -\vec{E}_d(\vec{r})\cdot\vec{P}$, where $\vec{E}_d = -\vec{\nabla}V_d$. The potential V_d represents a configuration of randomly placed dipoles,

$$V_d(\vec{r_i}) = \sum_j^{n_d} q_0(\vec{r_j})\Big[\frac{1}{|\vec{r_i} - (\vec{r_j} + \vec{\delta_j})|} - \frac{1}{|\vec{r_i} - (\vec{r_j} - \vec{\delta_j})|}\Big] \tag{6}$$

Here $q_0(\vec{r_j})$ and $\vec{\delta_j}$ represent the charge and the displacement, respectively, associated with the coarse-grained defect dipole centered at $\vec{r_j}$.

We assume that the system reaches mechanical equilibrium very fast so that we may integrate out the elastic fields, subject to the elastic compatibility constraint[8]. In terms of the strain components ϕ_1, ϕ_2 and ϕ_3, the elastic compatibility relation is given by

$$\nabla^2\phi_1 - (\frac{\partial^2}{\partial x^2} - \frac{\partial^2}{\partial y^2})\phi_2 - \sqrt{8}\frac{\partial^2}{\partial x \partial y}\phi_3 = 0. \tag{7}$$

The integration of the strain components, subject to the elastic compatibility constraints results in an effective long-range interaction for

the polarization field. For simplicity, we assume there is no contribution from the shear and bulk coupling, i.e, $q_1 \to 0$ and $q_2 \to 0$, then, the effective interaction in fourier space is given by

$$F_{eff} = \frac{{q_2}^2}{2a_2} \int d\vec{k} H(\vec{k}) |\Gamma(\vec{k})|^2, \tag{8}$$

where $H(\vec{k}) = (({h_1}^2(\vec{k})/\alpha) + {h_2}^2(\vec{k}) - 2h_2(\vec{k}) + ({h_3}^2(\vec{k})/\beta))$ and $\Gamma(\vec{k})$ is the fourier transform of ${P_x}^2 - {P_y}^2$. The quantities $h_1(\vec{k}) = k^2 Q(\vec{k})$, $h_2(\vec{k}) = [1 - ({k_x}^2 - {k_y}^2)Q(\vec{k})]$ and $h_3(\vec{k}) = -\sqrt{8} k_x k_y Q(\vec{k})$, with $Q(\vec{k})$ defined as

$$Q(\vec{k}) = \frac{({k_x}^2 - {k_y}^2)}{(k^4/\alpha + ({k_x}^2 - {k_y}^2)^2 + 8{k_x}^2{k_y}^2/\beta)}. \tag{9}$$

The constants $\alpha = a_1/a_2$ and $\beta = a_3/a_2$. The effective interaction derived above is strongly direction dependent and is crucial to determine the domain wall orientations. Similar anisotropic interactions have been considered in the context of martensitic transformations [9, 10].

Since we wish to address the issue of nucleation from defects, a dynamical formalism is needed to describe the non-equilibrium effects associated with domain switching. We introduce rescaled variables as follows: $t = (t^*/|\alpha_1|L)(\alpha_1 < 0)$, where L is the kinetic coefficient, $\vec{r} = (\phi x^*, \phi y^*)$ with $\phi = \sqrt{g_1/a|\alpha_1|}$, $b = (g_2/|\alpha_1|\phi^2)$,$c = (g_3/|\alpha_1|\phi^2)$; $P_x = P_R u$, $P_y = P_R v$, and $P_R = \sqrt{|\alpha_1|/\alpha_{11}}$. With this set of parameters, the TDGL equations are given by

$$\begin{aligned} u_{,t^*} &= u - u^3 - duv^2 + au_{,x^*x^*} + bu_{,y^*y^*} + cv_{,x^*y^*} + e_{x^*} + e_{x^*} \\ &\quad -\gamma u \int d\vec{k^*} H(\vec{k^*}) \Gamma(\vec{k^*}) exp(-\vec{k^*} \cdot \vec{r^*}) \\ v_{,t^*} &= v - v^3 - dvu^2 + av_{,y^*y^*} + bv_{,x^*x^*} + cu_{,x^*y^*} + e_{y^*} + e_{y^*} \\ &\quad +\gamma v \int d\vec{k^*} H(\vec{k^*}) \Gamma(\vec{k^*}) exp(-\vec{k^*} \cdot \vec{r^*}). \end{aligned} \tag{10}$$

Here, $\vec{e} = \vec{E}_{ext}/(P_R|\alpha_1|)$ is the rescaled external electric field and $\vec{\epsilon}$ is the rescaled electric field due to the defect dipoles, with $q_0(\vec{r}) = P_R\phi^2|\alpha_1| {q^*}_0(\vec{r^*})$. The constant $d = (\alpha_{12}/\alpha_{11})$ and $\gamma = ({g_2}^2/\alpha_{11}\phi^2 a_2)$.

In our simulations, equation (10) is discretized using finite differences on a 128×128 grid. The space discretization step $\Delta x^* = \Delta y^* = 1$

and the time interval $\Delta t^* = 0.02$. Periodic boundary conditions are applied in x and y directions, corresponding to a clamped infinite system. In order to compute the long-range terms in the equations, we have used pseudo-spectral method. The parameter values chosen for the simulations are $d = 0.5$ and $\gamma = 0.05$. The gradient coefficients are chosen as $a = b = c = 2$. Similarly, we choose the elastic parameters as $\alpha = \beta = 1$. For the defect field $\vec{\epsilon}$, we take $q^*{}_0$ to be uniformly distributed in the interval $[0.01, 0.03]$. The charge separation $\vec{\delta^*}$ can take value $(\pm c, 0)$ or $(0, \pm c)$, where c is a random number uniformly distributed in the interval $[0.08, 0.1]$. The switching behavior is studied by tuning the external electric field $\vec{E}_{ext}$. In this paper, we consider the applied external field only in the x direction, $\vec{e}_{ext} = (e_x, 0)$.

RESULTS

To study the time evolution of the domain patterns, we study switching behavior in steps. We first initialize the defect configuration by selecting random points on the grid. Then the electric field due to the defects is calculated at each grid pont. In the present work, we choose the number of defects as $n_d = 81 (\sim 0.5\%$ of the total points on the grid). Starting from random initial conditions, we choose a field $e_x = 18.2$ and simulate equation (10) for t^* up to 100. Very quickly, the system settles to a single domain state, with the polarization locally deviating from the equilibrium value in the vicinity of the defects. Using the single domain state as the initial condition, i.e. reset $t^* = 0$, the electric field is removed. In figure 1, we display the time evolution of the domain patterns following the field removal. In figure 1(a)($t^* = 2.5$), one can notice the appearance of polarization inhomogeneities at specific sites corresponding to dipolar defects. Some of the inhomogeneities evolve into domains with polarization orthogonal to the original direction of polarization. This nucleation and growth can be seen in figure 1(b) ($t^* = 7.5$) and figure 1(c)($t^* = 25$). Figure 1(d) shows the domain pattern at $t^* = 100$. Interestingly, we observe a twinned multi-domain state which has head to head as well as head to tail domain configurations. Our results are consistent with recent experiments, where charged domain walls have been observed[11]. It is believed that the charged domain walls may be stabilized by the charge defects.

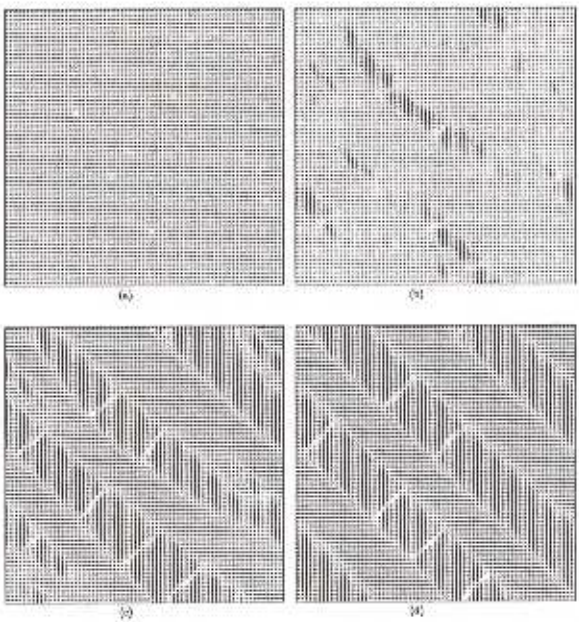

Figure 1: Time evolution of domain patterns following field removal from a single domain state. The time steps correspond to $t^* = 2.5$ (figure 1(a)), $t^* = 7.5$ (figure 1(b)), $t^* = 25$ (figure 1(c)), and $t^* = 100$ (figure 1(d)).

Because the periodic boundary conditions put a fixed volume constraint in the system, the minimum energy configuration is a 90^o twin-band, which can also be understood from the kernel of the elastic compatibility relations. The pre-existing nuclei can help to overcome the domain switching barrier and provide the seeds for the 90^o domains to form after the poling field is removed. The system is partially depoled due to the elastic constraints and the equilibrium state will have much reduced polarization. The depoling current may be estimated by the time derivative of the polarization, which is large at the beginning and gradually decreases to zero. In figures 2&3, we plot $< P_z >$ and I_x versus t^*, respectively. Both 90^o and 180^o twins exist at this stage. Next, we apply a field $e_x = -18$, which is larger than the

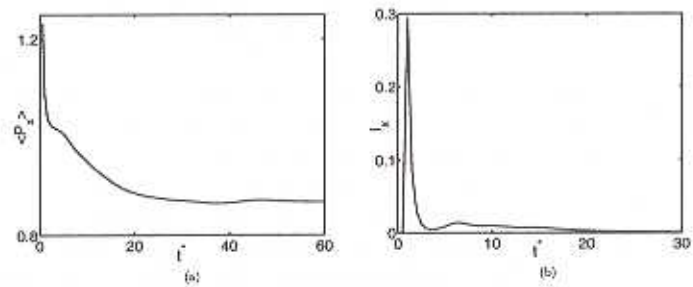

Figure 2: (a) Time dependence of $< P_x >$ for the situation shown in figure 1. (b) Time dependence of the simulated current I_x for the situation shown in figure 1. The current is calculated as $I_x = \frac{d < P_x >}{dt}$.

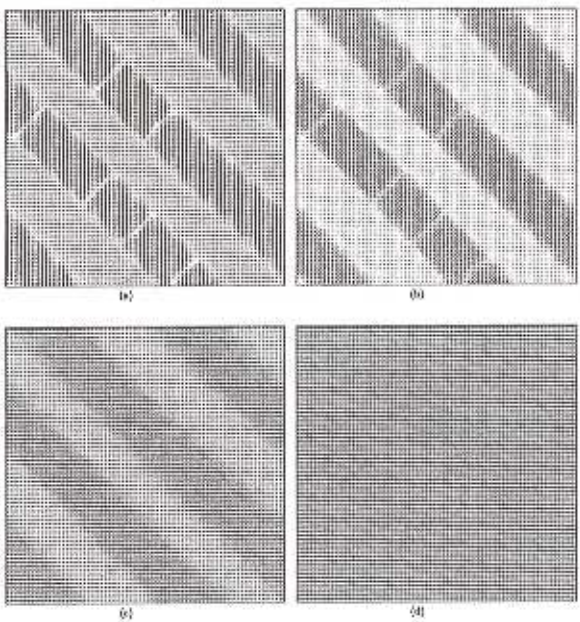

Figure 3: Time evolution of domain patterns following application of a field $e_x = -18.0$ to the multi-domain state of figure 1(d). The time steps correspond to $t^* = 0.04$ (figure 4(a)), $t^* = 0.08$ (figure 4(b)), $t^* = 0.24$ (figure 4(c)), and $t^* = 0.4$ (figure 4(d)).

coercive field, on the twinned multidomain state in figure 1(d). The subsequent switching process is displayed in figure 4. We can clearly see that the switching occurs by both 90° and 180° rotations in this case. To summarize, we have studied the time evolution of domain switching process in a ferroelectric system with dipolar defects using a time dependent-Ginzburg-Landau model. We find that the dipolar defects serve as nucleation centers for 90° twinned patterns, which generate back switching upon the removal of the poling field. The reverse switching of the multi-domain system could occur via both 90° and 180° dipolar rotations. Recent evidence for switching occurring by intermediate orthogonally polarized states has been recently observed in ultrasonic measurements on PZN-PT single crystals[12].

ACKNOWLEDGMENT

This research was sponsored by the Office of Naval Research.

References

[1] M. E. Lines and A. M. Glass,*Principles and Applications of Ferroelectrics and Related Materials* (Clarendon, Oxford, 1979).
[2] S. C. Hwang and G. Arlt, J. Appl. Phys., **87,** 869 (2000).
[3] Wenwu Cao, S. Tavener and S. Xie, J. Appl. Phys., **86,** 5793 (1999).
[4] S. Nambu and D.A. Sagala, Phys. Rev. B **50,** 5838 (1994).
[5] Hong-Liang Hu and Long-Qing Chen, Materials. Science. Engineering A **238,** 182 (1997).
[6] Rajeev Ahluwalia and Wenwu Cao (unpublished).
[7] Wenwu Cao and L. E. Cross, Phys. Rev. B **44,** 5 (1991).
[8] E. A. H. Love, *A Treatise on the Mathematical Theory of Elasticity* (Dover, New York, 1944), p. 49.
[9] S. Kartha, J. A. Krumhansl, J. P. Sethna and L. K. Wickham, Phys. Rev. B, **52,** 803 (1995).
[10] S. R. Shenoy, T. Lookman, A. Saxena and A. R. Bishop, Phys. Rev. B **60,** R12537 (1999).
[11] Jianhua Yin and Wenwu Cao, J. Appl. Phys. **87,** 7438 (2000).
[12] Wenwu Cao and Jianhua Yin (unpublished).